Taylor & Francis
Taylor & Francis Group

Estimating vegetation cover in an urban environment based on Landsat ETM+ imagery: A case study in Phoenix, USA

A. BUYANTUYEV*†‡, J. WU†‡ and C. GRIES‡

†School of Life Sciences, Arizona State University, Tempe, AZ 85287-4501, USA
‡Global Institute of Sustainability, Arizona State University, Tempe, AZ 85287-3211, USA

Studies of urban ecological systems can be greatly enhanced by combining ecosystem modelling and remote sensing which often requires establishing statistical relationships between field and remote sensing data. At the Central Arizona–Phoenix Long-Term Ecological Research (CAPLTER) site in the southwestern USA, we estimated vegetation abundance from Landsat ETM+ acquired at three dates by computing vegetation indices (NDVI and SAVI) and conducting linear spectral mixture analysis (SMA). Our analyses were stratified by three major land use/land covers—urban, agricultural, and desert. SMA, which provides direct measures of vegetation end member fraction for each pixel, was directly compared with field data and with the independent accuracy assessment dataset constructed from air photos. Vegetation index images with highest correlation with field data were used to construct regression models whose predictions were validated with the accuracy assessment dataset. We also investigated alternative regression methods, recognizing the inadequacy of traditional Ordinary Least Squares (OLS) in biophysical remote sensing. Symmetrical regressions—reduced major axis (RMA) and bisector ordinary least squares (OLS$_{bisector}$)—were evaluated and compared with OLS. Our results indicated that SMA was a more accurate approach to vegetation quantification in urban and agricultural land uses, but had a poor accuracy when applied to desert vegetation. Potential sources of errors and some improvement recommendations are discussed.

Keywords: Landsat ETM+; Urban; Vegetation index; Linear spectral mixture analysis; Regression analysis

1. Introduction

Urban development has profound effects on biodiversity and ecosystem functioning at local, regional, and global scales (Zipperer *et al.* 2000, Pickett *et al.* 2001). Phoenix, as one of the fastest growing metropolitan regions in the USA, provides striking examples of such land transformation (Jenerette and Wu 2001). The ongoing conversion of natural desert to an array of urban land cover types entails major ecological consequences that are yet to be fully understood (Baker *et al.* 2001, Wu and David 2002, Grimm and Redman 2004). Remote sensing data of various spatial, spectral, and temporal resolutions have been used to characterize land use

and land cover change associated with urban growth (Lunetta and Elvidge 1998, Lyon *et al.* 1998, Ridd and Liu 1998) and to derive biophysical variables driving ecosystem simulation models (Running *et al.* 1989, Ruimy *et al.* 1994, Running *et al.* 2000, Turner *et al.* 2004, Ustin *et al.* 2004). The latter application of remote sensing can greatly enhance our knowledge of urban ecological processes.

Spectral vegetation indices (SVI), such as the normalized difference vegetation index (NDVI), are traditional quantitative proxy measures of vegetation abundance or vigour, which are easy to compute and understand. However, such indices, when obtained using medium to coarse resolution multispectral satellite data, may introduce large errors into models that simulate landscapes with high spatial heterogeneity. Thus, more sophisticated methods for estimating vegetation abundance at the sub-pixel level have recently been developed (Adams *et al.* 1993, Adams *et al.* 1995, Hill and Hostert 1996, Phinn *et al.* 1999, Small 2001, Wu and Murray 2003, Lu and Weng 2004, Xiao *et al.* 2004). Several types of models for spectral mixture analysis (SMA) have been proposed, including linear, probabilistic, geometric and geometric-optical, stochastic geometric, and fuzzy models (Ichoku and Karnieli 1996). The commonly used linear spectral mixture analysis (SMA) decomposes a single pixel linearly into constituent land covers (end members) and obtains estimates of their areal fractions. It has been applied in different areas that are in demand of resolving the mixed pixel problem including arid lands (Smith *et al.* 1990, Roberts *et al.* 1993, Sohn and McCoy 1997, Elmore *et al.* 2000, McGwire *et al.* 2000, Asner 2004, Okin and Roberts 2004) and urbanized areas (Hill and Hostert 1996, Small 2001, Phinn *et al.* 2002, Rashed *et al.* 2003, Wu and Murray 2003, Liu and Weng 2004, Xiao *et al.* 2004). For urban applications in particular SMA has been shown to improve the accuracy of vegetation quantification considerably as compared to SVI. Besides being more accurate SMA is a meaningful approach because it provides a physically based measure of vegetation abundance.

A convenient ternary VIS (vegetation–impervious surface–soil) model developed by Ridd (1995) for urban areas has been applied in different urban settings using SMA on broadband imagery (Landsat). However, the VIS model has major drawbacks including its inability to adequately describe the complexity of urban surfaces present on the modelled scene. This can be mitigated by stratifying a study area into smaller regions or by using more end members. Mathematically the SMA in the latter situation is usually constrained by the number of spectral bands in the source data (Adams *et al.* 1986, Adams *et al.* 1993). Other solutions to the problem of multitude of urban land covers also exist (Roberts *et al.* 1998, Bateson *et al.* 2000, Rashed *et al.* 2003, Okin and Roberts 2004). Small (2001) concluded that in spite of the limited flexibility of broadband imagery to accommodate the heterogeneity of urban surfaces vegetation fraction accuracy in the three-end member model is still consistently high.

Establishing statistical relationship between vegetation characteristics acquired in the field and remotely sensed data is typically done by regression analysis with field data serving as dependent variables and various spectral vegetation indices (SVI) as independent variables (Price and Bausch 1995, Turner *et al.* 1999, Cohen *et al.* 2003). Ordinary least squares (OLS) has been the most frequently used method for relating the variables. Yet it has been well documented that OLS may be problematic when used in ecological (Sokal and Rohlf 1981, Seim and Saether 1983, LaBarbera 1989, Niklas 1994) and remote sensing (Curran and Hay 1986, Fernandes and Leblanc 2005) applications. One problem is the ambiguity in the

specification of the dependent Y (ground measured vegetation characteristics) versus independent X (remotely sensed signal) variable (Seim and Saether 1983, Curran and Hay 1986, Cohen *et al.* 2003). Although for practical purposes remotely sensed data is used to extrapolate the more expensive field data (dependent variable), reversing the variables is also possible. Secondly, OLS assumes that the independent variable is known without error but this assumption is rarely met in ecological or remote sensing studies because of measurement errors (Seim and Saether 1983, Curran and Hay 1986, LaBarbera 1989, Cohen *et al.* 2003). Therefore, Curran and Hay (1986) recommended two alternatives for cases where measurement error estimates for either X or Y are not available—reduced major axis (RMA) regression and Wald's method of groups. In contrast with OLS, RMA treats the two variables in the same way and it does not require that both variables were measured without an error term (LaBarbera 1989, Niklas 1994). It is just one of many possible lines between the OLS (Y on X) and inverse OLS (X on Y) (Cohen *et al.* 2003). RMA and OLS$_{bisector}$ (regression line that bisects the angle formed by the OLS and inverse OLS lines) regressions have been routinely used in biological allometry (McArdle 1988, Niklas 1994) and astronomy (Isobe and Feigelson 1990, Feigelson and Babu 1992). In remote sensing of ecosystem properties there is a real need for regression methods that treat variables symmetrically and make no assumption about relative amounts of measurement error (Cohen *et al.* 2003). There seems an emerging consensus among the remote sensing community that RMA is in general a more preferable method than OLS (Curran and Hay 1986, Babu and Feigelson 1992, Larsson 1993, Cohen *et al.* 2003). As an alternative to linear regression methods in remote sensing Fernandes and Leblanc (2005) recently suggested the use of a non-parametric (Theil-Sen) estimator.

The purpose of our study was to investigate the suitability of Landsat ETM + for estimating vegetative cover of the Greater Phoenix metropolitan area. We compare two distinct approaches to this problem: spectral vegetation indices (SVI) and linear spectral mixture analysis (SMA). To build statistical models that relate SVI to field measured vegetation cover we explore four types of regressions with theoretically different slope terms: the traditional ordinary least squares (OLS (Y on X)), the inverse OLS (X on Y), the OLS$_{bisector}$, and RMA.

2. Study area

The study area is the Central Arizona–Phoenix Long-Term Ecological Research (CAPLTER) site, which is centred at the city of Phoenix, Arizona, USA, within the northern part of the Sonoran Desert (figure 1). The landscape is dominated by a relatively flat terrain composed of alluvial plain and interrupted by eroded volcanic outcrops. Major drainage of the region is formed by the Gila and Salt Rivers. Agricultural activities have historically triggered a variety of water supply projects resulting in redistribution of water resources in space and time (Knowles-Yanez *et al.* 1999). Irrigation is the primary factor for sustaining managed vegetation in both agricultural and urban land uses. Local compositional variability of desert vegetation is remarkably high, due largely to variation in soil characteristics. Native vegetation is comprised of two subdivisions of the Sonoran desert scrub: Arizona Upland subdivision with Paloverde–Mixed Cacti series and Lower Colorado River subdivision with Creosotebush–Bursage series and formerly widespread Desert Saltbush (Turner 1974, Brown 1994). Managed vegetation types
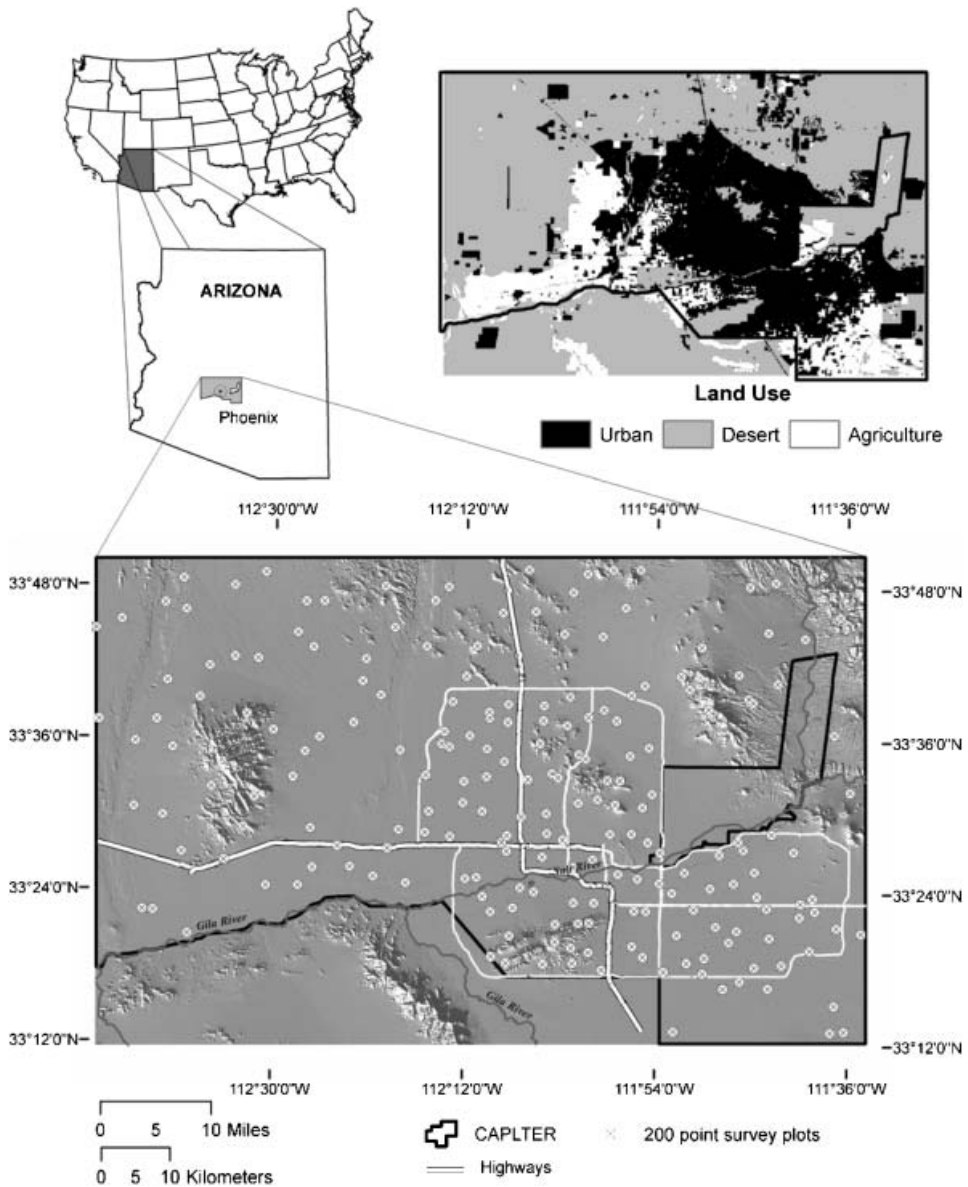
Figure 1.   Location of the study area and major land use types (200-point survey plots are not drawn to scale)

are also diverse, ranging from forest patches of coniferous or palm trees to backyard turf, golf courses, and agricultural fields. While a number of ecological and socio-economic studies have been carried out at CAPLTER (Grimm and Redman 2004), a grand challenge is to scale up information obtained at the local site level to landscape and regional levels (Wu and David 2002). This study is part of the effort to scale up ecosystem properties in the heterogeneous urban landscape using remote sensing data.

3. Data and methods

3.1 *Field data acquisition and post-processing*

From late February to early May of 2000, field data were collected in CAPLTER study area in 204 survey plots of 30×30 metres in size (figure 1). Plots were selected by means of a dual-density, randomized, and tessellation-stratified design with details described in (Hope *et al.* 2003, 2005, Grimm and Redman 2004). In each sampling plot all perennial plants were identified to genus, their locations recorded with GPS, and individual plant canopies measured along the two major axes (north–south and east–west).

Three major land use types were considered in grouping all plots: desert, agriculture, and urban (combined with transportation) (figure 1). In our analysis, we selected only those sites whose sampling was done within 1 month before or after each image's acquisition date which accounted for about half of the original plots. These three subsets were individually related to vegetation cover estimated with SMA and used in conducting regression analysis for SVI (table 1).

Field data were used to create vegetation maps and quantify vegetation cover for each plot. We used aerial photographs from 1997 (Digital Orthophoto Quarter Quadrangles and colour air photos) for mapping permanent structures in urban plots (e.g. buildings, parking lots and roads). GPS co-ordinates of individual perennial plants and their canopy cover measurements were used to generate a GIS layer of plant canopies in all urban plots. Elliptical crown shapes were assumed, and the total vegetation cover was then computed as a percentage of total plot surface area, which is assumed to be the prime determinant of remotely sensed signal of vegetation in the visible (VIS) and near-infrared (NIR) spectral regions (Graetz 1990). In desert plots only five individuals of each species were measured. We therefore estimated cover by multiplying species average (per plot) elliptical canopy by plant counts of a corresponding species recorded in the plot. Such approximation is prone to errors, but unfortunately no contemporaneous high-resolution remote sensing imagery was available to create accurate vegetation maps of desert plots. Instead we relied heavily on visual assessment and synoptic photographs taken at each site to crosscheck the resulting cover estimates. Finally, for agricultural plots we used visual field estimates of vegetation cover observed on dates the plots were visited.

3.2 *Image preprocessing*

Three Landsat Enhanced Thematic Mapper (ETM+) images (path 37/row 37) acquired under clear sky conditions on three dates (18 March, 19 April, and 21 May) from the year 2000 were used in the study. The nominal ground instantaneous field of view (IFOV) of the instrument is 30 metres which corresponds to the size of survey field plots. All images were georeferenced to the NAD 27 datum and UTM Zone 12 co-ordinate system. Due to high variability of vegetative cover over short distances and high risk of mismatch between field data and image data, we systematically checked the positional accuracy of the imagery and applied necessary geometric rectifications. We used a true colour aerial photo-mosaic (3 metre pixel, acquired in April of 1997) of the Phoenix metropolitan area and the Maricopa County street GIS map as reference sources. The image from March was first registered to the air photo using invariable features such as corners of rectangular agricultural fields and intersections of major roads with an estimated positional

Table 1. Frequency of surveyed field plots used in the analyses and Landsat imagery acquisition dates (the year is 2000).

	Urban	Desert	Agriculture
3 Feb	1		
7 Feb	3		
8 Feb	2		
9 Feb	1		
10 Feb			1
15 Feb	3		
16 Feb			1
17 Feb	2		
21 Feb	2		1
23 Feb	3		
24 Feb	1		2
29 Feb	1		1
1 Mar	3		
3 Mar	1		3
7 Mar	5		
8 Mar	3		1
10 Mar		1	
13 Mar	1		
14 Mar	4		
15 Mar	2		
16 Mar	4		
17 Mar	1	3	
March 18 Landsat image			
20 Mar	4		
21 Mar	1		3
22 Mar	2		1
23 Mar	4		1
24 Mar	2	1	
27 Mar		2	
28 Mar	4		
29 Mar			2
30 Mar		2	
31 Mar		3	1
3 Apr		3	
7 Apr		1	
10 Apr		3	
13 Apr		2	
14 Apr		2	
April 19 Landsat image			
20 Apr		2	
24 Apr		2	
25 Apr		2	
26 Apr		1	
27 Apr		2	
28 Apr		1	
1 May		1	
3 May		1	
4 May		2	
5 May		1	
9 May		1	

Table 1. (Continued).

	Urban	Desert	Agriculture
11 May		1	
12 May		2	
May 21 Landsat image			
Total	60	42	18

error of 0.5–1 pixel. The April and May images were then co-registered to the March one and subset to the extent of CAPLTER. Raw digital numbers (DN) were converted to radiance and then to exo-atmospheric reflectance units as specified in the Landsat handbook (Irish 1998). ATCOR2 module for ERDAS Imagine 8.6 (Geosystems 1997) was used to apply atmospheric corrections. For each dataset a mid-altitude summer, urban aerosol concentration model with 25 km estimated visibility was used as input to the MODTRAN3 radiative transfer code incorporated in the module.

3.3 *Vegetation indices*

Spectral vegetation indices (SVI) are based on the reflectance properties of green leaves that strongly absorb in red wavelengths and strongly reflect in near-infrared wavelengths. Many experimental studies have found varying sensitivities of different indices to potentially perturbing factors such as variation in soil background brightness, atmospheric turbidity, or sub-pixel vegetation structure variability (Huete and Jackson 1987, Jasinski 1990, Price and Bausch 1995, North 2002, Asner 2004). Because our study area embraces a variety of vegetative patch types including native desert plant communities and urban xeric to mesic vegetation, we found it appropriate to compute different indices that would allow comparison between them. Estimates of actively photosynthesizing vegetation abundance were obtained by deriving the two most frequently used and empirically tested indices: normalized difference vegetation index (NDVI) and soil adjusted vegetation index (SAVI) as shown below (Tucker 1979, Huete 1988, Jensen 1996):

$$NDVI = (NIR - RED)/(NIR + RED), \tag{1}$$

$$SAVI = [(NIR - RED)/(NIR + RED + L)/(1 + L)], \tag{2}$$

where *NIR* is Landsat band 4 (0.76–0.9 μm), *RED* is band 3 (0.63–0.69 μm), and *L* is the correction factor whose values range from 0 (high vegetation cover) to 1 (low vegetation). We used $L = 0.5$ in this study which was previously recommended by Huete (1988) and applied in land cover mapping of CAPLTER (Stefanov *et al.* 2001). Final values used in our study are the result of rescaling indices from 0 to 1 to avoid negative numbers.

3.4 *Spectral mixture analysis*

We implemented linear SMA which makes an assumption of insignificant non-linearity caused by multiple scattering. Mathematically the linear model is expressed

as (Smith *et al.* 1990, Adams *et al.* 1993, Settle and Drake 1993, Wu and Murray 2003)

$$x_b = \sum_{i=1}^{n} (f_i x_{i,b}) + e_b \text{ and } \sum_{i=1}^{n} f_i = 1 \ , \tag{3}$$

where x_b is normalized reflectance of each pixel in spectral band b; f_i is end member fraction; $x_{i,b}$ denotes normalized reflectance of i_{th} end member in band b; e_b is the error term; n is the number of end members. End member fractions can be solved by a least squares method which seeks minimization of the residual e_b provided the condition of independency of end members is met.

We first normalized the Landsat spectral bands as suggested by Wu (2004) and then transformed them to an orthogonal subset using minimum noise fraction (MNF) transformation (Green *et al.* 1988). MNF determines the inherent dimensionality and separates noise in data by whitening the noise covariance matrix followed by the standard Principal Component Analysis (ENVI 2000). The transformation yielded a plot of six final eigen values and coherent eigen images. The majority of spatially correlated variance was found in the low-order MNF components (typically first three), whereas the spatially uncorrelated variance was contained in higher order components. The second step was to identify potential end members. In the absence of spectral libraries for the area we utilized the pure pixel index (PPI) method (Boardman *et al.* 1995) which finds the most 'pure' pixels whose spectral properties signify end members. Two thousand iterations with the threshold of 2.5 were used to run the procedure. Most of identified pure pixels corresponded to croplands, golf courses, water bodies, and large buildings in the urban core. Not surprisingly very few pure pixels were found in desert. End members for SMA were selected by plotting pure pixel subsets of low order MNF components in n-D Visualizer—an interactive tool for locating, identifying, and clustering the most extreme spectral responses in a dataset (ENVI 2000). Distributions of transformed reflectances within the 3-D feature space suggested a four-component mixing model for all three dates (figure 2). The resulting end member spectra for all Landsat images were quite similar (figure 3). Once identified as green vegetation, water/ asphalt/shade (low albedo), and two high albedo surfaces including soil and rooftops, end member pixels were exported to the linear spectral unmixing algorithm that we applied to inverse MNF-transforms of low order eigen images. Four-end member models were inverted for end member fractions with the constrained option to force the output to sum to unity.

3.5 *Data sampling and regression analyses*

All Landsat-derived raster grids were sampled by overlaying them with sampling units (field plots) where each was divided into 100 subunits (lattice elements) as shown in figure 4. Landsat pixels were overlaid with lattice elements of a corresponding plot and then averaged. By taking this approach of weighted averaging we pursued a goal of accounting for situations where plot boundaries did not fall exactly onto a single Landsat pixel. The difference between these estimates and a simple average of 4 pixels can be significant (figure 4).

Because fraction images provide a direct measure of canopy cover we related them directly to field measured cover. SVI images, on the other hand, were used as independent variables in regression models that predicted field data. We used SAS
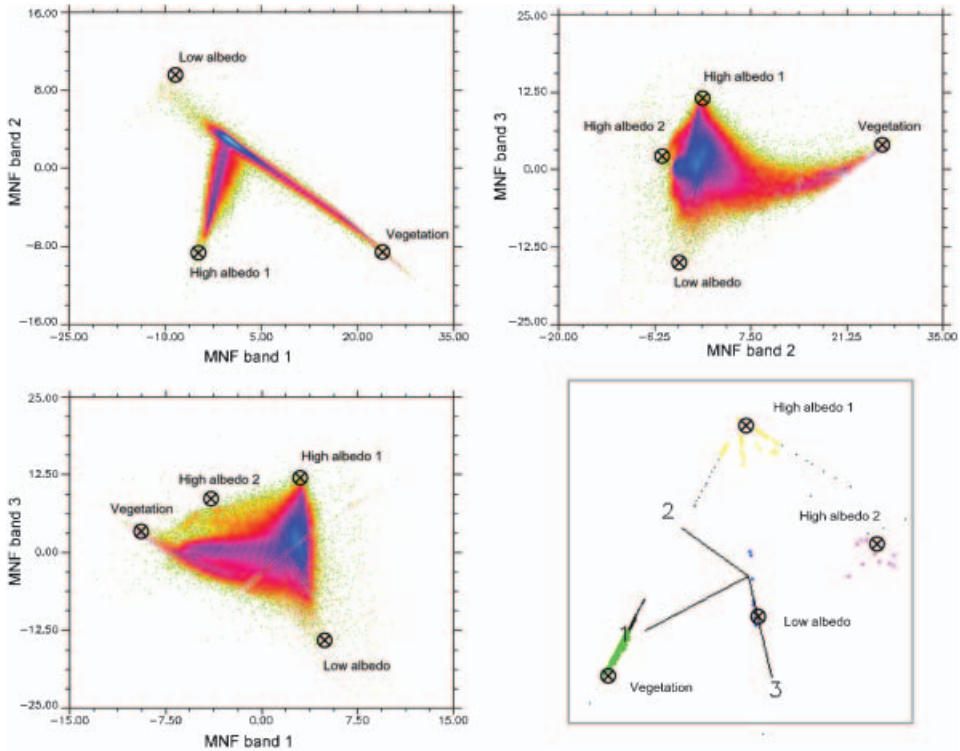
Figure 2. Transformed feature space representation of CAPLTER study area in March 18, 2000. The bottom right is the n-D visualization of the subset of spectrally pure pixels (from PPI) with painted extreme clusters representing end members. Three other graphs are density-slice scatter grams of the first three MNF components that contain the majority of the spatially correlated variance.

software to perform preliminary analyses of the data using standard OLS and checked for regression assumptions. Where necessary field measured cover (Y variable) was transformed based on suggestions of the Box-Cox procedure. We applied a square root transformation for urban and desert sites. Retransformations to the original scale were performed without bias correction and statistics were computed for back-transformed predictions. OLS, inverse OLS, OLS$_{bisector}$, and RMA regression models were computed using a modified program SLOPES available in the form of the Fortran computer code (http://ascl.net/slopes/slopes.f). Model computations were accompanied by uncertainty analysis based on numerical simulations and Bootstrap re-sampling (available as output of SLOPES) (Isobe and Feigelson 1990). Bootstrap uncertainty analysis is based on the distribution of slopes and intercepts of a large number of datasets constructed by random sampling of observed data with replacement.

We also used cross-validation as an additional means of comparing the models. The technique provides a virtually unbiased estimator of prediction error (Efron and Gong 1983). Discrete models were developed for each dataset and regression variant by deleting one observation at a time. Each model is then used to predict the observation that was left out. Predicted values were contrasted with actual observed cover. We compared models by computing variance ratios, root mean square errors (*RMSE*), and systematic errors (*SE*) as shown below:
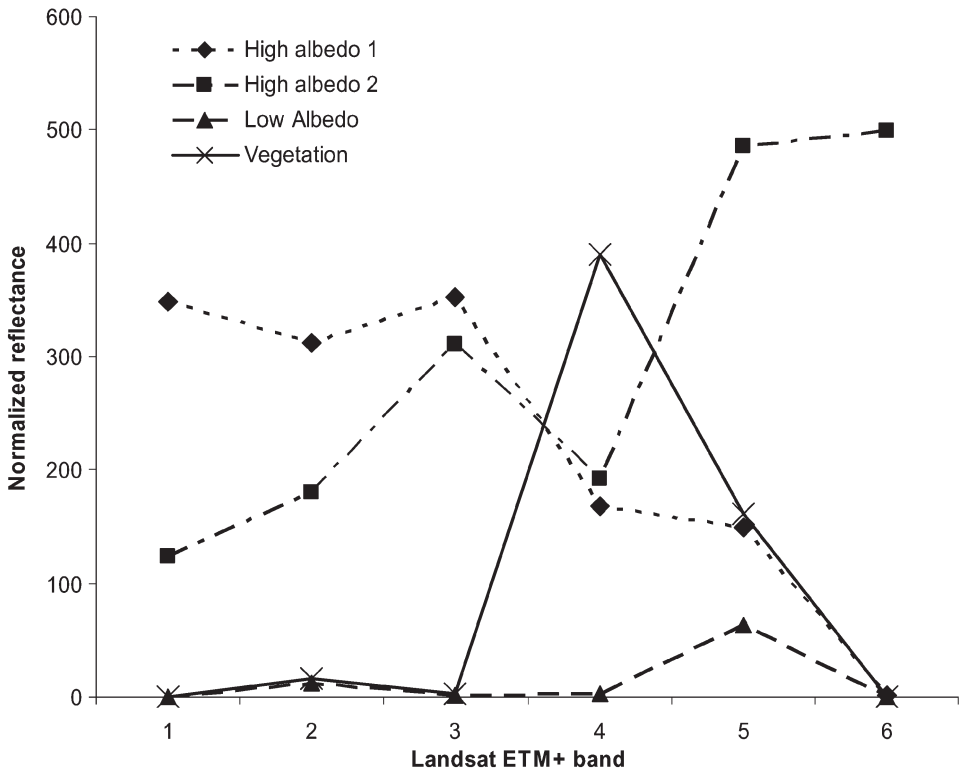
Figure 3.   End member reflectance spectra for 18 March 2000 used in spectral linear unmixing. The April and May plots are similar to the March one and hence not shown here.

$$\text{Variance ratio} = \widehat{\sigma}/\sigma \,, \tag{4}$$

$$RMSE = \sqrt{\frac{\sum\limits_{i=1}^{N} \left(\widehat{P}_i - P_i\right)^2}{N}} \,, \tag{5}$$

$$SE = \frac{\sum\limits_{i=1}^{N} \left(\widehat{P}_i - P_i\right)}{N} \,, \tag{6}$$

where $\widehat{\sigma}$, standard deviation of predicted values; σ, standard deviation of observed values; $\widehat{P}_i$, predicted cover for sample i; P_i, observed cover for sample i and N is the number of observations. *RMSE* measures the overall accuracy for all samples. Positive values of *SE* signify over-prediction, and negative values under-prediction. Finally, the variance ratio was used to evaluate how the variance changes with different models. A value close to one would indicate that the variance structure of observed values is preserved in predicted values (Cohen *et al.* 2003).

3.6   *Accuracy assessment*

Accuracy assessment was conducted by comparing cover predicted from regression models and vegetation fractions from SMA output with actual vegetation cover
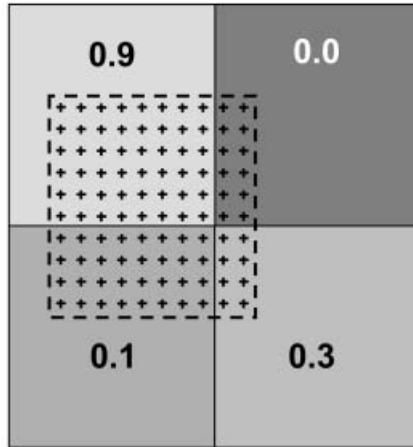
Average of 4 pixels $\dfrac{0.9 + 0 + 0.3 + 0.1}{4} = 0.3$

Average of 100 sampling units $\dfrac{0.9 * 48 + 0 * 12 + 0.3 * 8 + 0.1 * 32}{100} = 0.5$

Figure 4. Sampling Landsat for spatial regression analysis. Dotted boundary represents a survey plot converted into a lattice of 100 elements spaced at every 3 metres (crosses) and overlaid with 30 metre Landsat pixels (shaded squares). Displayed numbers are hypothetical NDVI and calculations below demonstrate differences between the two sampling schemes.

calculated from the true colour aerial photography (0.6 metre pixel size) acquired in April 2003. To get an independent sample we used an approach similar to that of Wu and Murray (2003). A stratified random sample of 200 validation sites 90×90 meters in size (nine Landsat pixels) was used. Sampling units bigger than one pixel were chosen to minimize possible geometric errors. One hundred sites were placed within urban land use, 50 within agricultural lands, and 50 in the desert. Each site was examined to ensure that it did not overlap with the survey plots and did not have a mixed land use. We also used the 1997 aerial photography to identify land use and land cover changes between 1997 and 2003. Some of the eliminated sites were found to be converted into urban land use; others revealed a significant difference in crop development. Subsequently 23 sites, mostly agricultural, were discarded. All sites were first classified into five classes by an iterative self-organizing data analysis (ISODATA) unsupervised method and converted into vector objects. We then employed a supervised approach by manually checking and reassigning values of the first two classes that typically represented vegetation (class 1) and asphalt/shade (class 2). Total area of patches of perennial vegetation (separated from shadows) was used to compute the total canopy cover. Percent vegetation cover was then compared with that estimated by SMA or regression models and averaged for nine Landsat pixels. Errors were assessed by *RMSE* and *SE* similarly to previously discussed measurements. Because these airborne data were collected in a different year we inspected scatter plots and checked correlations between the 250-metre MODIS NDVI images obtained to correspond in time to each of the Landsat images and 2003 air photo. Although a coarse estimate this gave us a general idea of how similar these rather large pixels were in terms of amount of vegetation.

4. Results

Vegetation index and vegetation fraction images for three dates are shown in figure 5. Root mean square (RMS) misfit images and corresponding statistics (not shown) produced along with end member fraction images were examined for any indication of large errors. Sufficiently low RMS (with a maximum of 10^{-5} and a mean of less than 10^{-6}) throughout the area suggested analytical validity of SMA model inversions. The images indirectly demonstrated phenological and structural changes in vegetation during the transition from early spring to early summer. We analysed them by computing NDVI difference between the three months. Vegetative cover underwent significant changes in croplands, developed urban area, and in riparian areas outside cities (NDVI increase>10%). Live vegetation cover rapidly increased from March to April in most of the Sonoran desert scrub and Arizona Upland and then decreased in May, suggesting an areal peak in live biomass sometime between late March and early May. Comparing March and May images revealed steadily increasing vegetative cover along the Gila and Verde Rivers, and decreasing overall cover throughout the CAPLTER site. To avoid potential errors that might occur in the plots selected for regression analysis due to spatiotemporal variation in cover, we sampled difference images to check for any significant change. No plots were discarded based on this criterion.

Pearson's correlation matrices (table 2) were used to select images with the highest agreement with actual vegetative cover. We also examined corresponding scatter plots for each pair of variables to confirm the relationships were linear. Our analysis suggested that desert plots would show better agreement with vegetation cover
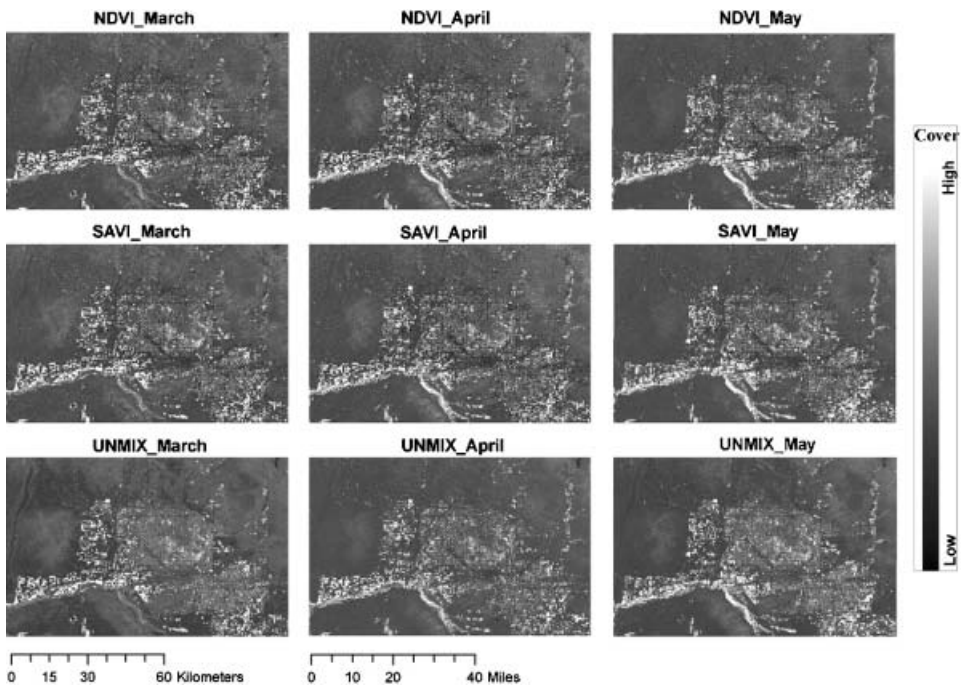
Figure 5. Vegetation indices and vegetation fraction images from SMA for all three dates. (NDVI and SAVI are spectral vegetation indices; UNMIX is vegetation fraction from SMA; Mar, March; Apr, April; May, May).

Table 2. Correlation of field measured vegetation cover with Landsat derived vegetation abundance.

	Desert vegetation	Urban vegetation	Agricultural vegetation
NDVI_Mar	0.42	0.70	0.99
SAVI_Mar	0.42	0.70	0.99
UNMIX_Mar	0.49	0.76	0.98
NDVI_Apr	0.67	0.51	0.95
SAVI_Apr	0.67	0.51	0.95
UNMIX_Apr	0.50	0.50	0.88
NDVI_May	0.53	0.58	0.53
SAVI_May	0.53	0.58	0.53
UNMIX_May	0.50	0.65	0.59

Notes: NDVI and SAVI are spectral vegetation indices, UNMIX is linearly unmixed vegetation.

computed from the April rather than March or May images. The highest correlation ($r=0.67$) was observed in April NDVI and SAVI. As expected NDVI ($r=0.70$), SAVI ($r=0.70$), and vegetation fraction ($r=0.76$) computed from March SMA were most closely correlated with field data in the urban area. Agricultural plots were also expected to correlate stronger with March image. Both March and April images were highly correlated with field data for agricultural plots. However, direct comparison of survey plots with accuracy assessment air photo showed that croplands in 2003 Landiscor photography had significantly higher agreement with April 2000 Landsat data. SAVI and NDVI were found essentially identical to each other for all three dates. NDVI as computationally simpler and widely used index was preferred. Consequently March NDVI image was used to build regression models for urban plots, and April NDVI image for desert and agricultural plots.

Differences in computed regression parameters of alternative models are obvious when fitted lines are shown on one graph (figure 6). The range of potential slopes is bounded by the two lines formed by OLS and inverse OLS. Effects of different modelling approaches are revealed when models are compared with respect to the statistics summarized in tables 3 and 4. In general, bootstrap simulations increase uncertainty of the slope term from OLS to OLS$_{bisector}$ and to RMA except the OLS$_{bisector}$ for agricultural land use. Urban and desert OLS and urban OLS$_{bisector}$ model were biased toward slight under-prediction (highest negative bias $SE=-0.027$). All agricultural models and urban and desert RMA were biased to over-prediction while OLS$_{bisector}$ for desert sites showed no bias ($SE=0$). Both symmetrical models (OLS$_{bisector}$ and RMA) produced a variance ratio close to one indicating that variance of the observed values is preserved in predicted values (Cohen *et al.* 2003). By design, OLS had the lowest *RMSE* (table 4). Despite its intermediate standard deviation of the slope term (table 3) OLS$_{bisector}$ provided a better fit for desert plots as reflected in higher correlation, low *RMSE*, variance ratio closest to unity, and no bias (table 4). However for urban plots no one model can be considered a clear winner. OLS had minimal uncertainty revealed in a small difference of the standard deviation of slope from the bootstrap slope. On the other hand it had the largest *SE* (tables 3 and 4). With its lowest uncertainty of regression parameters and lower RMSE and variance ratio, OLS was the best among regressions for agricultural land use.
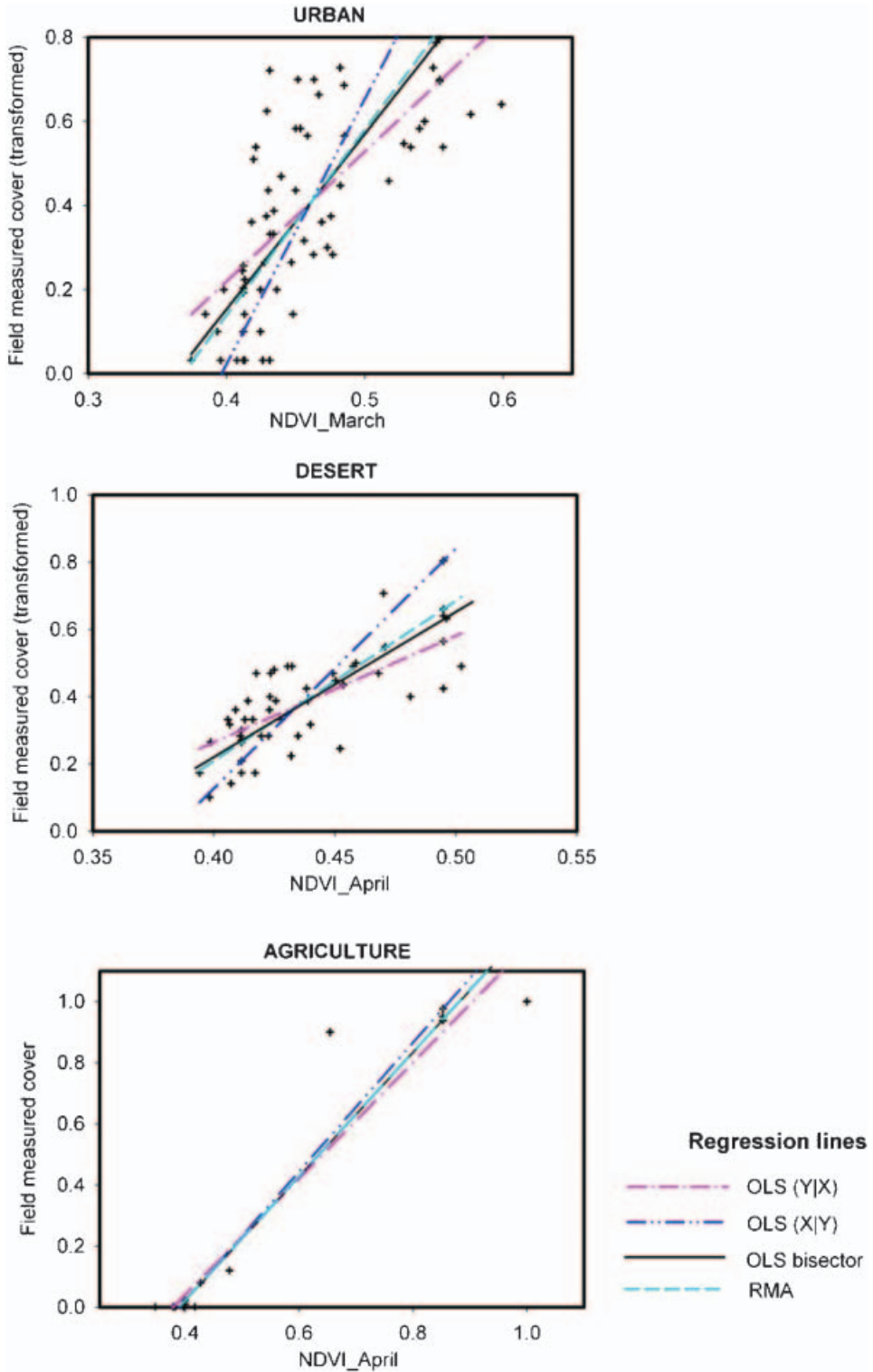
Figure 6. Scatter plots with fitted regression lines. Regression lines are explained in text and regression statistics are shown in table 3.

Table 3. Regression models with uncertainties. One standard deviation of regression parameters are shown in parentheses.

Dataset	Regression model	Analytical		Bootstrap slope	R^2
		Intercept	Slope		
Urban	OLS (Y|X)	−1.015 (±0.165)	3.087 (±0.348)	3.114 (±0.358)	0.57
(n=60)	OLS(X|Y)	−2.499 (±0.339)	6.306 (±0.775)	6.417 (±0.852)	0.57
	OLS$_{bisector}$	−1.515 (±0.168)	4.171 (±0.372)	4.198 (±0.391)	0.57
	RMA	−1.626 (±0.174)	4.412 (±0.393)	4.456 (±0.419)	0.57
Desert	OLS (Y|X)	−1.005 (±0.243)	3.172 (±0.559)	3.193 (±0.592)	0.45
(n=42)	OLS(X|Y)	−2.726 (±0.459)	7.133 (±1.075)	7.286 (±1.233)	0.45
	OLS$_{bisector}$	−1.549 (±0.254)	4.423 (±0.591)	4.428 (±0.632)	0.45
	RMA	−1.694 (±0.253)	4.757 (±0.591)	4.791 (±0.632)	0.45
Agricultural	OLS (Y|X)	−0.724 (±0.085)	1.907 (±0.220)	2.001 (±0.455)	0.91
(n=18)	OLS(X|Y)	−0.820 (±0.133)	2.107 (±0.334)	2.184 (±0.480)	0.91
	OLS$_{bisector}$	−0.770 (±0.105)	2.003 (±0.270)	2.087 (±0.463)	0.91
	RMA	− 0.771 (±0.105)	2.004 (±0.271)	2.088 (±0.465)	0.91

Notes: OLS (Y|X), ordinary least squares regression; OLS (X|Y), inverse ordinary least squares; OLS$_{bisector}$, bisector ordinary least squares; RMA, reduced major axis regression.

Table 4. Results of cross-validation for three regression models.

Dataset	Regression model	Variance ratio	R^2	RMSE	SE
Urban	OLS (Y|X)	0.698	0.68	0.159	−0.027
	OLS$_{bisector}$	0.951	0.69	0.189	−0.004
	RMA	1.008	0.69	0.200	0.003
Desert	OLS (Y|X)	0.685	0.62	0.082	−0.008
	OLS$_{bisector}$	0.964	0.64	0.094	0.000
	RMA	1.042	0.64	0.099	0.003
Agricultural	OLS (Y|X)	1.064	0.92	0.156	0.010
	OLS$_{bisector}$	1.122	0.92	0.165	0.010
	RMA	1.122	0.92	0.165	0.010

Abbreviations of regression models are explained in table 3.

Accuracy assessment suggested (table 5) that March vegetation fraction from SMA is the most accurate estimation of cover in urban and agricultural lands (figure 7). However SMA results did not show a good agreement for desert validation sites. Instead the April NDVI regressions provided a better estimation of which we chose to use OLS$_{bisector}$.

The composite map of vegetative cover (figure 8) was produced by combining three spatial subsets: March vegetation fraction from SMA for urban land use, OLS$_{bisector}$ predictions for April NDVI for desert, and April SMA derived fraction image for agricultural lands. Three different masks were imposed to apply these models to each of the corresponding land use types. The map depicts general patterns of vegetation in the metropolitan area reasonably well with peaks in cover associated with riparian areas, active croplands, and maintained urban vegetation communities.

Table 5. Accuracy assessment results of cover from selected SMA images and predicted by regressions using selected NDVI images.

Dataset	Source image	Regression model	R^2	RMSE	SE	N
Urban	UNMIX_MAR		0.70	0.055	0.003	
		OLS (Y|X)	0.32	0.142	0.072	87
	NDVI_MAR	OLS$_{bisector}$	0.30	0.210	0.099	
		RMA	0.30	0.227	0.107	
Desert	UNMIX_APR		0.32	0.047	− 0.029	
	NDVI_APR	OLS (Y|X)	0.44	0.005	0.016	
		OLS$_{bisector}$	0.41	0.007	0.016	60
		RMA	0.40	0.007	0.016	
Agricultural	UNMIX_APR		0.74	0.095	0.015	
	NDVI_APR	OLS (Y|X)	0.72	0.201	0.101	
		OLS$_{bisector}$	0.72	0.214	0.105	30
		RMA	0.72	0.214	0.105	

Abbreviations are explained in tables 2 and 3.

5.　Discussion and conclusions

Vegetation cover is an important input variable for building ecologically relevant land cover classifications that will enable us to develop a framework for linking
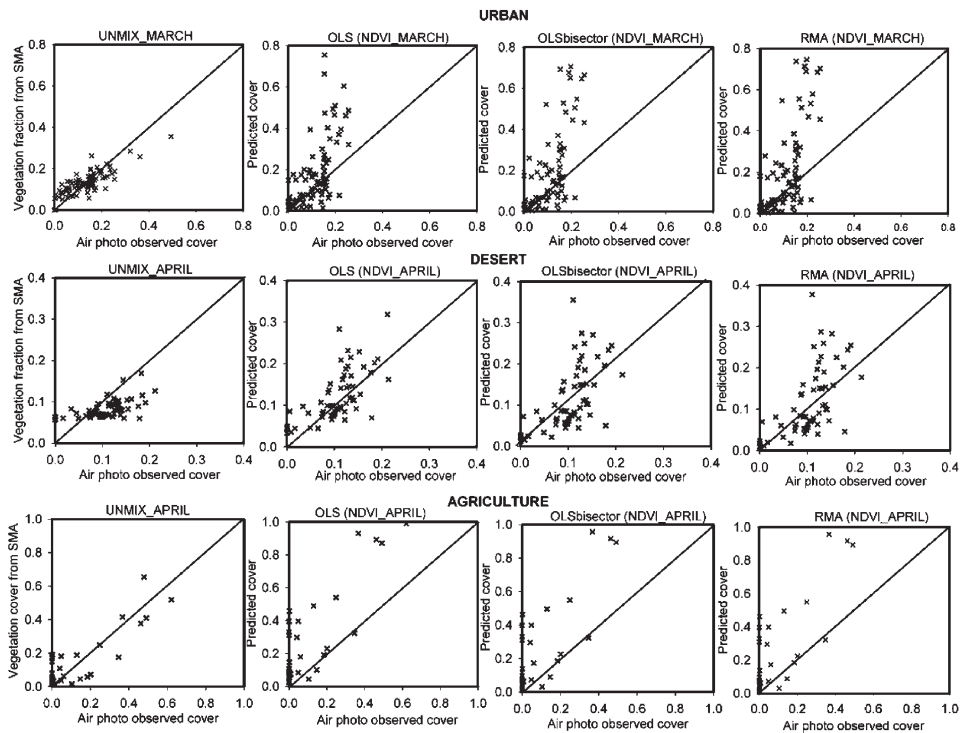

Figure 7.　Predicted versus observed (air photo classified validation sites) percent vegetation cover.
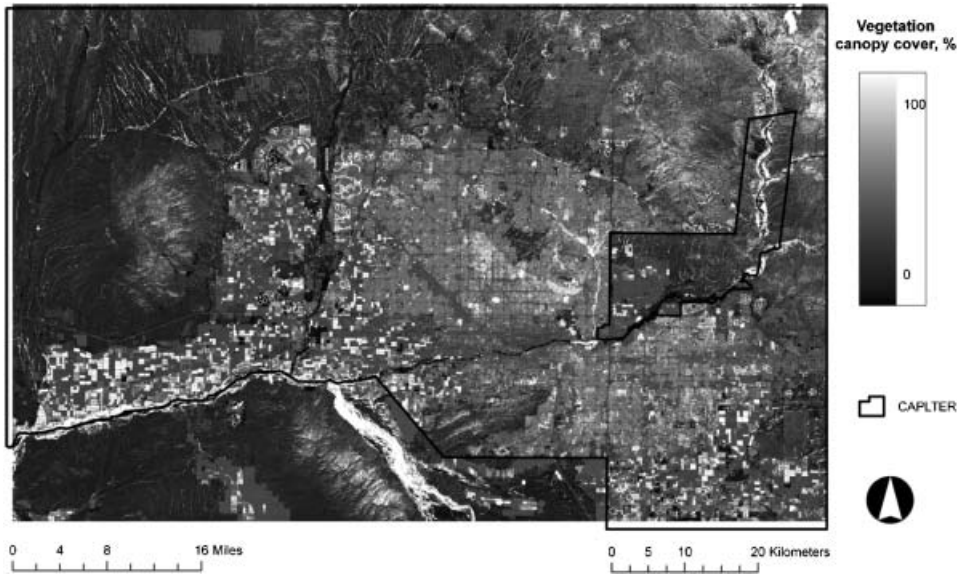
Figure 8. Composite map of vegetation cover in CAP LTER (Spring 2000). The map is created by applying three different estimators individually for each land use type.

remote sensing data to ecosystem process models of the urban landscape. The current study was motivated by the need to estimate vegetation cover in the rapidly urbanizing Phoenix using field data and Landsat ETM+ imagery. The secondary problem addressed in this study was the use of regression analysis in relating SVI to ground data.

Landsat data have been the best compromise solution for monitoring urban vegetation (Cohen and Goward 2004), but its coarse spatial resolution poses problems. As a result, computation of per-pixel vegetation indices and thematic classifications are likely to distort biomass/vegetative cover estimates. Spectral mixture analysis-based quantification of vegetation structure has been shown as a successful approach applied to urban environments (i.e. Small 2001, Phinn *et al.* 2002, Small 2002, Rashed *et al.* 2003, Wu and Murray 2003, Lu and Weng 2004). Our results also suggest that SMA was a more accurate method than SVI for mapping active green vegetation in the urban and agricultural landscapes of central Arizona, but it did not outperform SVI in the desert.

We identify several potential sources of errors in our analysis that can be categorized into the following:

1. Temporal inconsistencies in satellite and field data or of satellite and airborne validation data.
2. Measurement errors.
3. Errors in the end member selection process for SMA.
4. Geometric errors.

The order reflects the relative importance of these sources in the overall uncertainty.

We consider the mutual temporal mismatch between field data, satellite imagery, and air photos as a major source of uncertainty in our case study. Temporal incompatibility is likely to affect the accuracies of agricultural and desert plots that

exhibit considerable pattern dynamics (figure 5). Agricultural land use is ostensibly the most sensitive to temporal mismatch of the data because crop presence/absence on agricultural fields in the area is known to change frequently. Urban vegetation on the other hand has shown to be pseudo-invariant throughout the season studied herein. We eliminated the temporal inconsistency of our datasets by stratifying field plots by land use type and time of data collection; however the frequency of change in vegetation pattern in croplands still exceeds the chosen 1 month temporal threshold.

Measurement errors in our study refer mainly to inaccuracies in estimating vegetative cover in desert plots that are partially the result of temporal inconsistencies of data and field methods used. They are in our view a major cause of poor estimation of cover in desert plots. There are logistical limitations built in the design of the 200-point field survey stemming from the design of survey protocols aiming to collect as much data as possible for many different purposes within a reasonable time frame. It is important, however, to measure all individual trees and shrubs by either extending the protocol or conducting an additional sub-survey on desert sites. It is helpful to have timely high spatial resolution imagery used to map vegetation patches that can be verified in the field. Doing this should reduce measurement errors.

End member selection is a crucial step that affects the validity of SMA. Several methods have been proposed to narrow the set of suitable end members in highly complex landscapes (Bateson *et al.* 2000, Rashed *et al.* 2003, Lu and Weng 2004). Since SMA shows promise to improve vegetation mapping in urbanizing central Arizona, further efforts will be needed to decide on what strategy will perform best here. We believe that the low accuracy of desert vegetation classification can be improved if a spectral library of major desert land covers is collected and used instead of image derived end members. Spectral limitations of SMA developed from broadband sensors such as Landsat should also be recognized.

Geometric errors are always an issue when merging different scales in an analysis. Urban landscapes are very sensitive to spatial mis-registration because abrupt changes in land cover are often below the spatial resolution of Landsat. Although we rigorously checked the accuracy of all ETM+ images uncertainty in positional accuracy could still be a problem considering the large extent of the study area.

We used regression analysis to relate field data to NDVI images. While the choice of regression method to use was not critical for urban and agricultural lands desert land cover required analysis of uncertainties associated with regressions because accuracy for SMA was low. The comparison of different regression methods involved computation of several regression lines and uncertainty analysis. Our results indicate that OLS developed for desert plots resulted in the highest accuracy. However, the attenuation of original variance in OLS predictions may become a source of additional errors (Cohen *et al.* 2003). Moreover unnecessary output errors are produced if predicted biophysical variables are used to drive simulation models. These problems are aggravated if correlation between these variables and sensor data is sufficiently low. Symmetrical regressions such as RMA and OLS$_{bisector}$ are alternatives that help to reduce these uncertainties although at the expense of other errors such as those expressed in *RMSE*. More importantly, though uncertainties can be minimized in OLS by rigorous statistical tests, regression analysis theory suggests that applying OLS in many biophysical remote sensing applications is flawed in principle. We used OLS$_{bisector}$ to predict desert vegetation because of its

overall less uncertainty although it had lower than OLS accuracy when compared with the validation dataset.

We conclude that overall SMA is a more accurate approach to quantitative measures of vegetation that can be used in various research activities within CAPLTER including land cover and land use classifications, evaluation of urban heat island effects, and correlation of socio-economic variables with ecosystem processes in the Phoenix metro area (Stefanov *et al.* 2001, Baker *et al.* 2002, Hawkins *et al.* 2004, Shochat *et al.* 2004). All these projects would benefit from more detailed and more accurate account of the spatio-temporal structure of vegetation.

References
ADAMS, J.B., MILTON, M.O. and GILLESPIE, A.R., 1993, Imagine spectroscopy: Interpretation based on spectral mixture analysis. In *Remote Geochemical Analysis: Elemental and Mineralogical Composition*, C.M. Pieters and P.A.J. Englert, (Eds), pp. 145–166 (New York: Cambridge University Press).

ADAMS, J.B., SABOL, D.E., KAPOS, V., FILHO, R.A., ROBERTS, D.A., SMITH, M.O. and GILLESPIE, A.R., 1995, Classification of multispectral images based on fractions of endmembers: Application to land-cover change in the Brazilian Amazon. *Remote Sensing of Environment*, **52**, pp. 137–154.

ADAMS, J.B., SMITH, M.O. and JOHNSON, P.E., 1986, Spectral mixture modeling: A new analysis of rock and soil types at the Viking Lander 1 site. *Journal of Geophysical Research*, **91**, pp. 8098–8112.

AKRITAS, M.G. and BERSHADY, M.A., 1996, Linear regression for astronomical data with measurement errors and intrinsic scatter. *Astrophysical Journal*, **470**, pp. 706–714.

ASNER, G.P., 2004, Biophysical remote sensing signatures of arid and semiarid ecosystems. In *Remote Sensing for Natural Resource Management and Environmental Monitoring: Manual of Remote Sensing*, S.L. Ustin (Ed.), pp. 53–109 (New York: John Wiley & Sons).

BABU, G.J. and FEIGELSON, E.D., 1992, Analytical and Monte Carlo comparisons of six different linear least squares fits. *Communications in Statistics: Simulation and Computation*, **21**, pp. 533–549.

BAKER, L.A., BRAZEL, A.J., SELOVER, N., MARTIN, C.A., MCINTYRE, N.E., STEINER, F.R., NELSON, A.L. and MUSACCHIO, L., 2002, Urbanization and warming of Phoenix (Arizona, USA): Impacts, feedbacks, and mitigation. *Urban Ecosystems*, **6**, pp. 183–203.

BAKER, L.A., HOPE, D., XU, Y., EDMONDS, J. and LAUVER, L., 2001, Nitrogen balance for the Central Arizona-Phoenix (CAP) ecosystem. *Ecosystems*, **4**, pp. 582–602.

BATESON, A., ASNER, G.P. and WESSMAN, C.A., 2000, Endmember bundles: A new approach to incorporating endmember variability in spectral mixture analysis. *IEEE Transactions on Geoscience and Remote Sensing*, **38**, pp. 1083–1094.

BOARDMAN, J.W., KRUSE, F.A. and GREEN, R.O., 1995, Mapping target signatures via partial unmixing of AVIRIS data. In *Fifth JPL Airborne Earth Science Workshop*, pp. 23–26.

BROWN, D.E., 1994, *Biotic Communities: Southwestern United States and Northwestern Mexico*, pp. 342 (Salt Lake City: University of Utah Press).

COHEN, W.B. and GOWARD, S.N., 2004, Landsat's role in ecological applications of remote sensing. *BioScience*, **54**, pp. 535–545.

COHEN, W.B., MAIERSPERGER, T.K., GOWER, S.T. and TURNER, D.P., 2003, An improved strategy for regression of biophysical variables and Landsat ETM+ data. *Remote Sensing of Environment*, **84**, pp. 561–571.

CURRAN, P.J. and HAY, A.M., 1986, The importance of measurement error for certain procedures in remote sensing at optical wavelengths. *Photogrammetric Engineering and Remote Sensing*, **52**, pp. 229–241.

EFRON, B. and GONG, G., 1983, A leisurely look at the bootstrap, the jackknife, and cross-validation. *The American Statistician*, **37**, pp. 36–48.

ELMORE, A.J., MUSTARD, J.F., MANNING, S.J. and LOBELL, D.B., 2000, Quantifying vegetation change in semiarid environments: Precision and accuracy of spectral mixture analysis and the normalized difference vegetation index. *Remote Sensing of Environment*, **73**, pp. 87–102.

ENVI 2000, ENVI User's Guide, Research Systems Inc.

FEIGELSON, E.D. and BABU, G.J., 1992, Linear regression in Astronomy. II. *Astrophysical Journal*, **397**, pp. 55–67.

FERNANDES, R. and LEBLANC, S.G., 2005, Parametric (modified least squares) and non-parametric (Theil-Sen) linear regressions for predicting biophysical parameters in the presence of measurement errors. *Remote Sensing of Environment*, **95**, pp. 303–316.

GEOSYSTEMS,, 1997, *ATCOR2 for ERDAS Imagine User Manual*, GmbH (Ed.) (Germany: Germering).

GRAETZ, R.D., 1990, Remote sensing of terrestrial ecosystem structure: An ecologist's pragmatic view. In *Remote Sensing of Biosphere Functioning*, R.J. Hobbs and H.A. Mooney, (Eds), pp. 5–30 (New York and Berlin: Springer-Verlag).

GREEN, A.A., BERMAN, M., SWITZER, P. and CRAIG, M.D., 1988, A transformation for ordering multispectral data in terms of image quality with implications for noise removal. *IEEE Transactions on Geoscience and Remote Sensing*, **26**, pp. 65–74.

GRIMM, N.B. and REDMAN, C.L., 2004, Approaches to the study of urban ecosystems: The case of Central Arizona-Phoenix. *Urban Ecosystems*, **7**, pp. 199–213.

HAWKINS, T.W., BRAZEL, A., STEFANOV, W., BIGLER, W. and SAFFELL, E.M., 2004, The role of rural variability in urban heat island and oasis determination for Phoenix, Arizona. *Journal of Applied Meteorology*, **43**, pp. 476–486.

HILL, J. and HOSTERT, P., 1996, Monitoring the growth of Mediterranean metropolis based on the analysis of spectral mixtures—a case study of Athens (Greece). In *Progress in Environmental Remote Sensing Research and Applications*, E. Parlow (Ed.), pp. 21–31 (Rotterdam: A.A. Balkema).

HOPE, D., GRIES, C., ZHU, W., FAGAN, W.F., REDMAN, C.L., GRIMM, N.B., NELSON, A.L., MARTIN, C.A. and KINZIG, A., 2003, Socioeconomics drive urban plant diversity. *Proceedings of the National Academy of Sciences*, **100**, pp. 8788–8792.

HOPE, D., ZHU, W., GRIES, C., OLESON, J., KAYE, J., GRIMM, N.B. and BAKER, B., 2005, Spatial variation in soil inorganic nitrogen across and arid urban ecosystem. *Urban Ecosystems*, **8**, pp. 251–273.

HUETE, A.R., 1988, A soil-adjusted vegetation index (SAVI). *Remote Sensing of Environment*, **25**, pp. 295–309.

HUETE, A.R. and JACKSON, R.D., 1987, Suitability of spectral Indices for evaluating vegetation characteristics on arid rangelands. *Remote Sensing of Environment*, **23**, pp. 213–232.

ICHOKU, C. and KARNIELI, A., 1996, A review of mixture modeling techniques for sub-pixel land cover estimation. *Remote Sensing Reviews*, **13**, pp. 161–186.

IRISH, R., 1998, Data product. Landsat 7 science data use handbook (Greenbelt, MD: Goddard Space Flight Center). Available online at: http://ltpwww.gsfc.nasa.gov/IAS/handbook/handbook_htmls/chapter11/chapter11.html (accessed 20 July 2005).

ISOBE, T. and FEIGELSON, E.D., 1990, Linear regression in Astronomy. I. *Astrophysical Journal*, **364**, pp. 104–113.

JASINSKI, M.F., 1990, Sensitivity of normalized difference vegetation index to subpixel canopy cover, soil albedo, and pixel scale. *Remote Sensing of Environment*, **32**, pp. 169–187.

JENERETTE, G.D. and WU, J., 2001, Analysis and simulation of land-use change in the central Arizona-Phoenix region, USA. *Landscape Ecology*, **16**, pp. 611–626.

JENSEN, J.R., 1996, *Introductory Digital Image Processing: A Remote Sensing Perspective*, 2nd edn (Upper Saddle River, NJ: Prentice Hall).

KNOWLES-YANEZ, K., MORITZ, C., FRY, J., REDMAN, C.L., BUCCHIN, M. and MCCARTNEY, P.H., 1999, *Historic Land Use: Phase I Report on Generalized Land Use*, Central Arizona-Phoenix Long-Term Ecological Research, Arizona State University.

LABARBERA, M., 1989, Analyzing body size as a factor in ecology and evolution. *Annual Reviews of Ecology and Systematics*, **20**, pp. 97–117.

LARSSON, H., 1993, Linear regression for canopy cover estimation in Acacia woodlands using Landsat-TM, -MSS and SPOT HRV XS data. *International Journal of Remote Sensing*, **14**, pp. 2129–2136.

LU, D. and WENG, Q., 2004, Spectral mixture analysis of the urban landscape in Indianapolis with Landsat ETM + imagery. *Photogrammetric Engineering and Remote Sensing*, **70**, pp. 1053–1062.

LUCK, M. and WU, J., 2002, A gradient analysis of urban landscape pattern: A case study from the Phoenix metropolitan region, Arizona, USA. *Landscape Ecology*, **17**, pp. 327–339.

LUNETTA, R.S. and ELVIDGE, C.D., 1998, *Remote Sensing Change Detection: Environmental Monitoring Methods and Applications*, 318 pp. (Chelsea, MI: Ann Arbor Press).

LYON, J.G., YUAN, D., LUNETTA, R.S. and ELVIDGE, C.D., 1998, A change detection experiment using vegetation indices. *Photogrammetric Engineering and Remote Sensing*, **64**, pp. 143–150.

MCARDLE, B.H., 1988, The structural relationship: Regression in biology. *Canadian Journal of Zoology*, **66**, pp. 2329–2339.

MCGWIRE, K., MINOR, T. and FENSTERMAKER, L., 2000, Hyperspectral mixture modeling for quantifying sparse vegetation cover in arid environments. *Remote Sensing of Environment*, **72**, pp. 360–374.

NIKLAS, K.J., 1994, *Plant Allometry: The Scaling of Form and Process* (Chicago: University of Chicago Press).

NORTH, P.R.J., 2002, Estimation of fAPAR, LAI, and vegetation fractional cover from ATSR-2 imagery. *Remote Sensing of Environment*, **80**, pp. 114–121.

OKIN, G.S. and ROBERTS, D.A., 2004, Remote sensing of arid regions: Challenges and opportunities. In *Remote Sensing For Natural Resource Management and Environmental Monitoring: Manual of Remote Sensing*, S.L. Ustin (Ed.), pp. 111–145 (New York: John Wiley & Sons).

PHINN, S.R., STANFORD, M. and SCARTH, P., 2002, Monitoring the composition of urban environments based on the vegetation-impervious-soil (VIS) model by subpixel techniques. *International Journal of Remote Sensing*, **23**, pp. 4131–4153.

PHINN, S.R., STOW, D. and VAN MOUWEIRK, D., 1999, Remotely sensed estimates of vegetation structural characteristics in restored wetlands, Southern California. *Photogrammetric Engineering and Remote Sensing*, **65**, pp. 485–493.

PICKETT, S.T.A., CADENASSO, M.L., GROVE, J.M., NILON, C.H., POUYAT, R.V., ZIPPERER, W.C. and COSTANZA, R., 2001, Urban ecological systems: Linking terrestrial ecological, physical, and socioeconomic components of metropolitan areas. *Annual Review of Ecology and Systematics*, **32**, pp. 127–157.

PRICE, J.C. and BAUSCH, W.C., 1995, Leaf Area Index estimation from visible and near-infrared reflectance data. *Remote Sensing of Environment*, **52**, pp. 55–65.

RASHED, T., WEEKS, J., ROBERTS, D.A., ROGAN, J. and POWELL, P., 2003, Measuring the physical composition of urban morphology using multiple endmember spectral

mixture models. *Photogrammetric Engineering and Remote Sensing*, **69**, pp. 1011–1020.

REICH, P.B., TURNER, D.P. and BOLSTAD, P., 1999, An approach to spatially distributed modeling of Net Primary Production (NPP) at the landscape scale and its application in validation of EOS NPP products. *Remote Sensing of Environment*, **70**, pp. 69–81.

RIDD, M.K., 1995, Exploring a V-I-S (vegetation-impervious surface-soil) model for urban ecosystem analysis through remote sensing: comparative anatomy of cities. *International Journal of Remote Sensing*, **16**, pp. 2165–2185.

RIDD, M.K. and LIU, J., 1998, A comparison of four algorithms for change detection in an urban environment. *Remote Sensing of Environment*, **63**, pp. 95–100.

ROBERTS, D.A., GARDNER, M.E., CHURCH, R., USTIN, S.L., SCHEER, G. and GREEN, R.O., 1998, Mapping chaparral in the Santa Monica Mountains using multiple endmember spectral mixture models. *Remote Sensing of Environment*, **65**, pp. 267–279.

ROBERTS, D.A., SMITH, M.O. and ADAMS, J.B., 1993, Green vegetation, nonphotosynthetic vegetation and soils in AVIRIS data. *Remote Sensing of Environment*, **44**, pp. 255–269.

RUIMY, A., SAUGIER, B. and DEDIEU, G., 1994, Methodology for the estimation of terrestrial net primary production from remotely sensed data. *Journal of Geophysical Research*, **99**, pp. 5263–5383.

RUNNING, S.W., NEMANI, R.R., PETERSON, D.L., BAND, L.E., POTTS, D.F., PIERCE, L.L. and SPANNER, M.A., 1989, Mapping regional forest evapotranspiration and photosynthesis by coupling satellite data with ecosystem simulation. *Ecology*, **70**, pp. 1090–1101.

RUNNING, S.W., THORNTON, P.E., NEMANI, R.R. and GLASSY, J.M., 2000, Global terrestrial gross and net primary productivity from the Earth Observing System. In *Methods in Ecosystem Science*, O.E. Sala, R.B. Jackson, H.A. Mooney and R.W. Howarth, (Eds), pp. 44–57 (New York: Springer-Verlag).

SEIM, E. and SAETHER, B.-E., 1983, On rethinking allometry: which regression model to use? *Journal of Theoretical Biology*, **104**, pp. 161–168.

SETTLE, J.J. and DRAKE, N.A., 1993, Linear mixing and the estimation of ground cover proportions. *International Journal of Remote Sensing*, **14**, pp. 1159–1177.

SHOCHAT, E., STEFANOV, W.L., WHITEHORSE, M.E. and FAETH, S., 2004, Urbanization and spider diversity: Influences of human modification of habitat structure and productivity. *Ecological Applications*, **14**, pp. 268–280.

SMALL, C., 2001, Estimation of urban vegetation abundance by spectral mixture analysis. *International Journal of Remote Sensing*, **22**, pp. 1305–1334.

SMALL, C., 2002, Multitemporal analysis of urban reflectance. *Remote Sensing of Environment*, **81**, pp. 427–442.

SMITH, M.O., USTIN, S.L., ADAMS, J.B. and GILLESPIE, A.R., 1990, Vegetation in deserts: I. A regional measure of abundance from multispectral images. *Remote Sensing of Environment*, **31**, pp. 1–26.

SOHN, Y. and MCCOY, R.M., 1997, Mapping desert shrub rangeland using spectral unmixing and modeling spectral mixtures with TM data. *Photogrammetric Engineering and Remote Sensing*, **63**, pp. 707–716.

SOKAL, R.R. and ROHLF, F.J., 1981, *Biometry: The Principles and Practice of Statistics in Biological Research*, 2nd edn (San Francisco, CA: W.H. Freeman).

STEFANOV, W.L., RAMSEY, M.S. and CHRISTENSEN, P.R., 2001, Monitoring urban land cover change: An expert system approach to land cover classification of semiarid to arid urban centers. *Remote Sensing of Environment*, **77**, pp. 173–185.

STUCKENS, J., COPPIN, P.R. and BAUER, M.E., 2000, Integrating contextual information with per-pixel classification for improved land cover classification. *Remote Sensing of Environment*, **71**, pp. 282–296.

TUCKER, C.J., 1979, Red and photographic infrared linear combinations for monitoring vegetation. *Remote Sensing of Environment*, **8**, pp. 127–150.

TURNER, D.P., COHEN, W.B., KENNEDY, R.E., FASSNACHT, K.S. and BRIGGS, J.M., 1999, Relationships between Leaf Area Index and Landsat TM spectral vegetation indices across three temperate zone sites. *Remote Sensing of Environment*, **70**, pp. 52–68.

TURNER, D.P., OLLINGER, S.V. and KIMBALL, J.S., 2004, Integrating remote sensing and ecosystem process models for landscape and regional scale analysis of the carbon cycle. *BioScience*, **54**, pp. 573–584.

TURNER, R.M., 1974, Map showing vegetation in the Phoenix area, Arizona: Miscellaneous investigations series, U.S. Geologic Survey, Map I-845-I.

USTIN, S.L., ROBERTS, D.A., GAMON, J.A., ASNER, G.P. and GREEN, R.O., 2004, Using imaging spectrometry to study ecosystem processes and properties. *BioScience*, **54**, pp. 523–534.

WU, C., 2004, Normalized spectral mixture analysis for monitoring urban composition using ETM+ imagery. *Remote Sensing of Environment*, **93**, pp. 480–492.

WU, C. and MURRAY, A.T., 2003, Estimating impervious surface distribution by spectral mixture analysis. *Remote Sensing of Environment*, **84**, pp. 493–505.

WU, J. and DAVID, J.L., 2002, A spatially explicit hierarchical approach to modeling complex ecological systems: Theory and applications. *Ecological Modelling*, **153**, pp. 7–26.

XIAO, Q., USTIN, S.L. and MCPHERSON, E.G., 2004, Using AVIRIS data and multiple-masking techniques to map urban forest tree species. *International Journal of Remote Sensing*, **25**, pp. 5637–5654.

ZIPPERER, W.C., WU, J., POUYAT, R.V. and PICKETT, S.T.A., 2000, The application of ecological principles to urban and urbanizing landscapes. *Ecological Applications*, **10**, pp. 685–688.